



1 of 1

 [Download](#)  [Print](#)  [Save to PDF](#)  [Save to list](#)  [Create bibliography](#)*Chemical Physics Impact* • Open Access • Volume 7 • December 2023 • Article number 100347**Document type**

Article • Gold Open Access

**Source type**

Journal

**ISSN**

26670224

**DOI**

10.1016/j.chphi.2023.100347

[View more](#) 

# Metal-doped fullerenes as promising drug carriers of hydroxycarbamide anticancer: Insights from density functional theory

Salem-Bekhit M.M.<sup>a</sup>; Al Zahrani S.<sup>a</sup>; Alhabib N.A.<sup>a</sup>;Maaliw III R.R.<sup>b</sup>; Da'i M.<sup>c</sup> ; Mirzaei M.<sup>d</sup> [Save all to author list](#)<sup>a</sup> Kayyali Chair for Pharmaceutical Industries, Department of Pharmaceutics, College of Pharmacy, King Saud University, PO Box 2457, Riyadh, 11451, Saudi Arabia<sup>b</sup> College of Engineering, Southern Luzon State University, Quezon, Lucban, Philippines<sup>c</sup> Faculty of Pharmacy, Universitas Muhammadiyah Surakarta, Surakarta, Indonesia<sup>d</sup> Laboratory of Molecular Computations (LMC), Department of Natural and Mathematical Sciences, Faculty of Engineering, Tarsus University, Tarsus, Turkey

3 86th percentile

Citations in Scopus

2.12

FWCI

[View all metrics >](#)[Full text options](#) [Export](#) 

Cited by 3 documents

Density functional theory assessments of an iron-doped graphene platform towards the hydrea anticancer drug delivery

Saadh, M.J. , Mirzaei, M. , Dhiaa, S.M. (2024) *Diamond and Related Materials*

Explorations of structural and electronic features of an enhanced iron-doped boron nitride nanocage for adsorbing/sensing functions of the hydroxyurea anticancer drug delivery under density functional theory calculations

Saadh, M.J. , Mirzaei, M. , Abdullaeva, B.S. (2023) *Physica B: Condensed Matter*

Computational assessments of sumanene-hydroxyurea conjugations for proposing a novel drug design and delivery platform

Saadh, M.J. , Mirzaei, M. , Ahmed, H.H. (2023) *Chemical Physics Impact*

[View all 3 citing documents](#)

Inform me when this document is cited in Scopus:

[Set citation alert >](#)

## Related documents

An Iron-enhanced nanocone assisted drug delivery of Aspirin: DFT assessments

Ghasemi Gol, A. , Akbari, J. , Khalaj, M. (2023) *International Journal of Nano Dimension*

A facile detection of ethanol by the Be/Mg/Ca-enhanced fullerenes: Insights from density functional theory

Toiserkani, F. , Mirzaei, M. , Alcan, V. (2023) *Chemical Physics Impact*

Density functional theory assessments of an iron-doped graphene platform towards the hydrea anticancer drug delivery

Saadh, M.J. , Mirzaei, M. , Dhiaa, S.M. (2024) *Diamond and Related Materials*

[View all related documents based on references](#)

Find more related documents in Scopus based on:

[Authors >](#) [Keywords >](#)

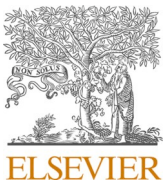
**Abstract****Author keywords****Sustainable Development Goals 2023****SciVal Topics****Metrics****Funding details****SciVal Topics****Metrics****Funding details****Abstract**

Assessing an idea of metal-doped fullerenes (MF) as promising drug carriers of hydroxycarbamide; also known as hydroxyurea, (Hyd) anticancer was done in this work by performing density functional theory (DFT) calculations. A model of carbon fullerene was doped by each of iron (Fe), nickel (Ni), and zinc (Zn) transition metal atoms to provide enhanced FeF, NiF, and ZnF doped fullerenes for working towards the Hyd anticancer regarding the drug delivery issues. The model were optimized and their evaluated features indicated a possibility of occurrence of MF → Hyd@MF mechanism through the involving O...M and H...C interactions from the Hyd side to the MF side. The longest recovery time duration was supposed to be found for the Hyd@ZnF complex because of the largest strength and the highest conductance rate variation was supposed to be found for the Hyd@NiF complex because of the smallest energy gap. However, all the complex models were in a reasonable level of formations and electronic variations to be monitored for approaching a sensing or detecting function. In this regard, the enhanced models of FeF, NiF, and ZnF doped fullerenes were found suitable to work as promising carriers of Hyd anticancer regarding the drug delivery issues by the formation of interacting Hyd@FeF, Hyd@NiF, and Hyd@ZnF complexes in meaningful levels of structural and electronic features. © 2023 The Author(s)

**Author keywords**

Adsorption; Cancer; Drug delivery; Drug interaction; Molecular simulation

[Sustainable Development Goals 2023](#) [New](#)[SciVal Topics](#)



## Full Length Article

# Metal-doped fullerenes as promising drug carriers of hydroxycarbamide anticancer: Insights from density functional theory

M.M. Salem-Bekhit <sup>a</sup>, S. Al Zahrani <sup>a</sup>, N.A. Alhabib <sup>a</sup>, R.R. Maaliw III <sup>b</sup>, M. Da'i <sup>c,\*</sup>, M. Mirzaei <sup>d</sup>

<sup>a</sup> Kayyali Chair for Pharmaceutical Industries, Department of Pharmaceutics, College of Pharmacy, King Saud University, PO Box 2457, Riyadh 11451, Saudi Arabia

<sup>b</sup> College of Engineering, Southern Luzon State University, Lucban, Quezon, Philippines

<sup>c</sup> Faculty of Pharmacy, Universitas Muhammadiyah Surakarta, Surakarta, Indonesia

<sup>d</sup> Laboratory of Molecular Computations (LMC), Department of Natural and Mathematical Sciences, Faculty of Engineering, Tarsus University, Tarsus, Turkey

## ARTICLE INFO

**Keywords:**  
Adsorption  
Cancer  
Drug delivery  
Drug interaction  
Molecular simulation

## ABSTRACT

Assessing an idea of metal-doped fullerenes (MF) as promising drug carriers of hydroxycarbamide; also known as hydroxyurea, (Hyd) anticancer was done in this work by performing density functional theory (DFT) calculations. A model of carbon fullerene was doped by each of iron (Fe), nickel (Ni), and zinc (Zn) transition metal atoms to provide enhanced FeF, NiF, and ZnF doped fullerenes for working towards the Hyd anticancer regarding the drug delivery issues. The model were optimized and their evaluated features indicated a possibility of occurrence of MF → Hyd@MF mechanism through the involving O...M and H...C interactions from the Hyd side to the MF side. The longest recovery time duration was supposed to be found for the Hyd@ZnF complex because of the largest strength and the highest conductance rate variation was supposed to be found for the Hyd@NiF complex because of the smallest energy gap. However, all the complex models were in a reasonable level of formations and electronic variations to be monitored for approaching a sensing or detecting function. In this regard, the enhanced models of FeF, NiF, and ZnF doped fullerenes were found suitable to work as promising carriers of Hyd anticancer regarding the drug delivery issues by the formation of interacting Hyd@FeF, Hyd@NiF, and Hyd@ZnF complexes in meaningful levels of structural and electronic features.

## 1. Introduction

Drug design, discovery, development, and delivery ( $D_5$ ) is indeed a very complex process dealing with several restricting factors in regarding the biochemical systems [1–3]. Accordingly, several attempts have been done to recognize details of such complex systems by determining the roles of multi-counterparts for working in a successful process [4–6]. The human body is indeed a very mixed system requiring so many efforts to learn its details for dealing with it in a successful treatment [7–9]. In the case of medications, so many bio-related protocols, information, and materials are required to overcome the diseases or to save the health level [10–12]. Especially in the case of mediations by drugs and external materials, delivering the substance to the correct target is a real challenging area [13–15]. To this aim, providing a suitable carrier has been seen very important for pushing forward the drug delivery platform to carry the drug in a controlled level [16–18]. Hence, those structures with characteristic surface features have been seen very useful to work as possible carriers of drug delivery platforms, in which

the nano-materials have been as the most important candidates of this area [19–21]. After the pioneering innovation of carbon nanotubes, the research efforts have focused on the determination of the novel nano-materials for customizing into different purposes [22–24]. As mentioned about the importance of emerging needs for maintaining the health issues, considerable efforts have been dedicated to recognize the bio-related applications of nano-materials such as their use in the drug delivery platforms [25–27]. Hence, the current work was focused on the determination of a category of metal-doped fullerenes for working as promising drug carriers of hydroxycarbamide anticancer along with density functional theory (DFT) calculations. Indeed, the quantum chemical DFT calculations could provide very useful insights into the details of modified complex structures avoiding the existence of any interferers [28–30]. In this regard, the current work was done based on the evaluated structural and electronic features of hydroxycarbamide and metal-doped fullerenes in the singular and bimolecular states (Fig. 1) to recognize the impacts of complex formations on the future features of involving counterparts for developing their applications.

\* Corresponding author.

E-mail address: muhammad.dai@ums.ac.id (M. Da'i).

Hydroxycarbamide (Hyd); also known as hydroxyurea, is an anti-metabolite chemotherapy drug stopping the cancer cells making and repairing to inhibit their growth and multiplication with a vital role in treating some of cancer types such as chronic myeloid leukemia, head, and neck cancer [31,32]. Additionally, preventing the painful symptoms and reducing the blood transfusions need in patients with sickle cell anemia were done under the Hyd treatment [33,34]. However, arising the side effects limited the Hyd treatment under a very careful medication and protocol [35,36]. To this point, providing a new drug delivery platform could help to overcome the unwanted effects of Hyd by enhancing its efficiency for the targeted medication purposes [37–39]. The earlier works indicated the importance of nanostructures for making interacting complexes with the Hyd drug to bring a possible drug carrier

platform [40–44]. Accordingly, an idea of assessing metal-assisted fullerenes (MF) as promising carriers of Hyd anticancer drug was done in this work to provide new insights into the development of corresponding drug delivery platforms. Hence, the existence of any communication between the Hyd and MF counterparts was examined using the DFT calculations to show the occurrence of adsorption process in the Hyd@MF complexes. Indeed, the metal-doping enhancement could bring new structural and electronic features to the nanostructures by providing more activated surface for participating in the adsorption and interaction processes [45–47]. As shown in Fig. 1, a model of carbon fullerene structure was decorated by each of Fe (iron), Ni (nickel), and Zn (zinc), transition metal atoms to yield the enhanced MF counterpart. The idea of employing metal-nano-particle (MNP) substances has a rich

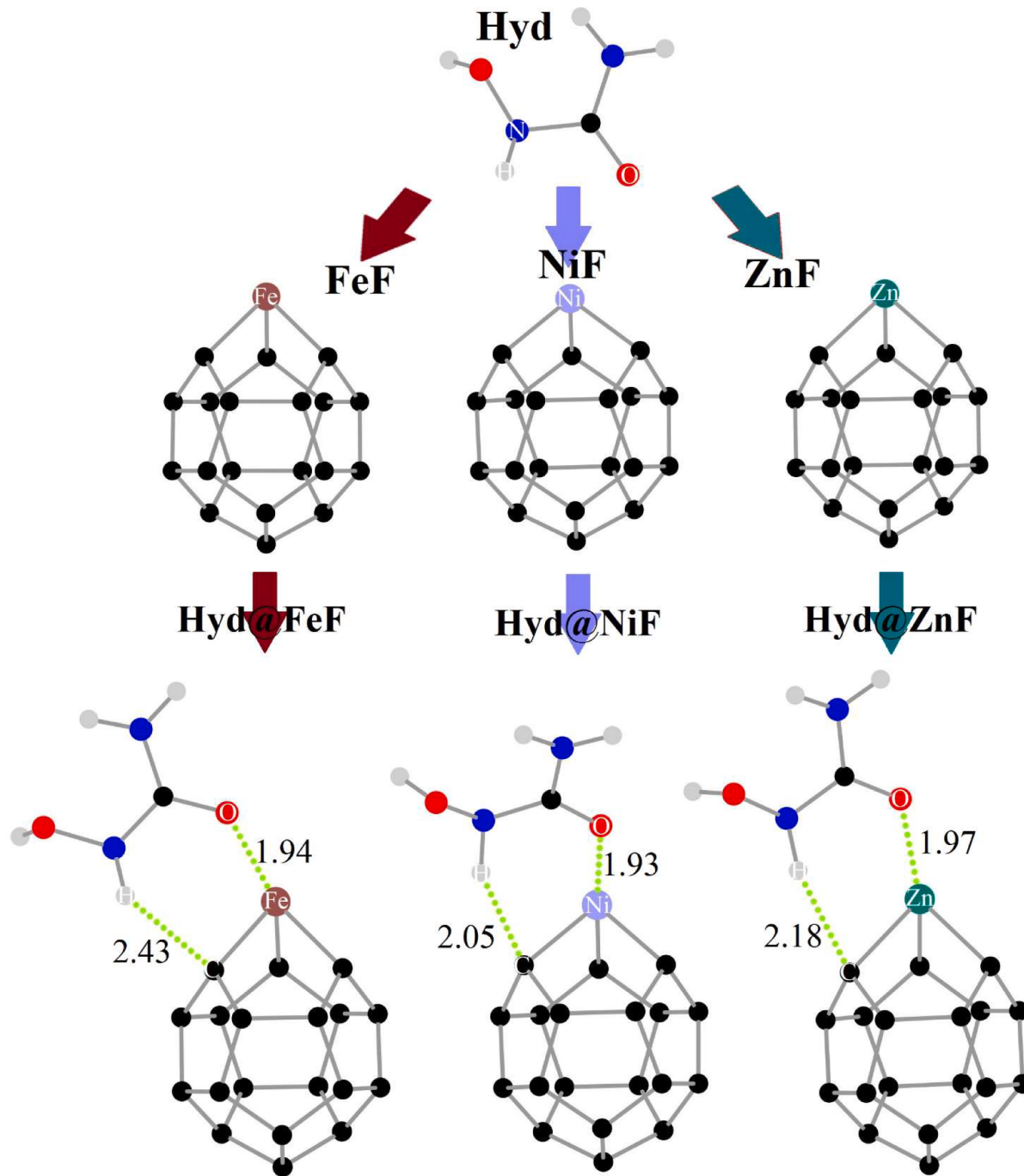


**Fig. 1.** The Optimized models of this work; including the singular Hyd and MF models and the interacting Hyd@MF complexes. The green dotted-line interaction distances were written in Å. (For interpretation of the references to color in this figure legend, the reader is referred to the web version of this article.)

history in the literature showing their suitability of working in various fields of biological related systems [48]. Especially in the case of interactions, the metal-doped nanostructures showed advantages of managing the interacting region to yield more efficient complex formations due to the molecular communications [49–51]. Accordingly, such a remarkable advantage was examined in this work by employing the MF substance for the drug delivery of Hyd anticancer through the formation of Hyd@MF complexes (Fig. 1). The obtained quantitative and graphics of this work were summarized in Tables 1–3 and Figs. 1 and 2. It is important to mention that the investigations on cancer topics are very important because of a lack of enough success to overcome this issue [52–55]. Herein, the current work was done for customizing a model of molecular systems for approaching the drug delivery purposes of Hyd anticancer by the assistance of MF particles.

## 2. Materials and methods

The investigated models of this work including the singular Hyd ( $\text{CH}_4\text{N}_2\text{O}_2$ ) and MF ( $\text{MC}_{19}$ ) counterparts and their Hyd@MF complexes were shown in Fig. 1. For making the MF models, one carbon atom of a  $\text{C}_{20}$  fullerene was substituted by each of Fe, Ni, and Zn, transition metal atoms to produce the enhanced FeF, NiF, and ZnF doped fullerenes. Earlier works indicated a suitability of  $\text{C}_{20}$  fullerene for employing in the adsorption studies and also drug delivery investigations for representing the fullerene structures in the computation outlook [49,50,56,57]. The geometries of singular models were optimized to obtain their stabilized conformations. Next, the combinations of already optimized conformers of Hyd and MF were re-optimized to yield Hyd@MF complexes including Hyd@FeF, Hyd@NiF, and Hyd@ZnF models. The involving interactions between Hyd and MF counterparts were recognized by performing additional analyses of quantum theory of atoms in molecules (QTAIM) [58,59]. Subsequently, the total energy values of singular and complex states were compared to each other by including the effects of basis set superposition error (BSSE) [60] to yield the strength of integration energy between the counterparts as indicated by  $E_{\text{int}}$ . The results of QTAIM analyses and  $E_{\text{int}}$  of optimized models (Fig. 1) were summarized in Table 1. Next, the models were analyzed based on the obtained thermochemistry features including the sum of electronic and thermal free energies ( $E + G$ ), the sum of electronic and thermal enthalpies ( $E + H$ ), and the entropy ( $S$ ) (Table 2). Further assessments of models were based on the evaluation of frontier molecular orbital (FMO) properties to reveal the electronic features of singular and complex states. To this aim, energy values of the dominant FMO levels; including the highest occupied molecular orbital (HOMO) and the lowest unoccupied molecular orbital (LUMO), were calculated and their related features; including the values of energy gap ( $E_{\text{gap}}$ ), chemical potential ( $C_{\text{pot}}$ ) and chemical hardness ( $C_{\text{hard}}$ ), were evaluated (Table 3). Furthermore, distribution patterns of HOMO and LUMO and diagrams of density of states (DOS) were exhibited in Fig. 2 to make sense the variations of electronic features among the singular and complex states. The results of this work were obtained by performing M06-2X/6-31G\* level of DFT calculations using the Gaussian program [61–63]. After performing the DFT calculations, the Multiwfn [64] program was used for the QTAIM results

extraction, the GaussSum [65] program was used for the DOS diagrams illustrations, and the ChemCraft [66] program was used for visualizing the models structures and HOMO and LUMO patterns of this work.

## 3. Results and discussion

By the importance of developing novel drug delivery platforms especially for the cancer treatments, the current work was done to assess benefits of metal-doped fullerenes (MF) as promising carriers of hydroxycarbamide; also known as hydroxyurea, (Hyd) anticancer. The geometries of 3D molecular models were optimized by performing DFT calculations, and their corresponding structural and electronic features were evaluated. In the case of Hyd model, it should be noted that the molecular relaxation depends on its customization for involving in interactions with another substance, in which other possible conformational structures could be also found for it [67]. To create the MF models, one of Fe, Ni, and Zn transition metal atoms were used for substituting one carbon atom of a  $\text{C}_{20}$  fullerene to make a  $\text{MC}_{19}$  metal-doped fullerene as indicated by MF. As a result, three MF models were created and their geometries were stabilized to be peppered for interacting with the already optimized Hyd substance. Next, combinations of Hyd and each of MF models were re-optimized to obtain the Hyd@MF complexes (Fig. 1). To do this, different starting orientations of interactions by various sides of Hyd and MF counterparts were examined, in which the final results were found for the investigation of this work. The main idea was achieving the physically interacting complex models; the results were in a confirmation level of affirming this idea as recognized by additional QTAIM analyses. Accordingly, the stability of complexes and their detailed interaction environments were assessed to reveal what has been happening inside the complex systems. In this regard, the already stabilized configurations of Hyd@MF complexes were assessed based on the QTAIM features (Table 1) to recognize the involving interactions and their features.

Generally, two non-covalent interactions were found for the formation of each complex; including O...M and H...C interactions from the Hyd side to the MF side. By the variation of M atom, different properties were found and the final configurations of counterparts towards each other in the complexes were clarified. Based on the distances between Hyd and MF counterparts, the Hyd@NiF complex was at the shortest distance and the Hyd@ZnF complex was at the longest distance; however, both of O...M and H...C interactions were significant for all three complexes. Recognizing the properties of interactions by the QTAIM features, the models were found to be in strong interactions with the strongest ones for the Hyd@ZnF complex. The evaluated values of QTAIM features; including  $\rho$  (total electron density),  $\nabla^2\rho$  (Laplacian of electron density), and  $H$  (energy of electron density), indicated that the O...M integration was stronger than the H...C interaction in the complex models. In the case of O...M interaction, Zn showed the highest significant role for interacting with the O atom of Hyd, and Ni and Fe were placed at the next levels. In the case of H...C interaction, again the Zn-doped model showed the highest significant role of a neighboring C atom for interacting with the H atom of Hyd, and Ni- and Fe-doped models were placed at the next levels. So it could be assumed that the significance of formation of Hyd@MF complexes could be arranged by  $\text{Hyd@ZnF} > \text{Hyd@NiF} > \text{Hyd@FeF}$  complexes.

To better affirm this achievement, the values of  $E_{\text{int}}$  were obtained as  $-34.59$  kcal/mol,  $-35.64$  kcal/mol, and  $-36.82$  kcal/mol, for the Hyd@FeF, Hyd@NiF, and Hyd@ZnF complexes. In this regard, formations of the complex models were confirmed by the assistance of detailed information of QTAIM features and the evaluated values of  $E_{\text{int}}$ . It is worth to mention that a recovery time duration could be directly related to the strength of complex formation, in which a stronger complex could lead to a longer recovery time duration. To this point, all three complexes were found applicable to approach a meaningful recovery time with the highest significance of Hyd@ZnF complex. The results of stabilities could be summarized a significant role of metal-doping atom for

**Table 1**  
The evaluated QTAIM features and  $E_{\text{int}}$  of interacting Hyd@MF complexes.\*

Hyd@MF	Interaction	Distance (Å)	$\rho$ (au)	$\nabla^2\rho$ (au)	H (au)	$E_{\text{int}}$ (kcal/mol)
Hyd@FeF	O...Fe	1.94	0.073	0.38	-0.045	-34.59
	H...C	2.43	0.013	0.039	0.0014	
Hyd@NiF	O...Ni	1.93	0.075	0.39	-0.046	-35.64
	H...C	2.05	0.028	0.061	-0.0022	
Hyd@ZnF	O...Zn	1.97	0.083	0.41	-0.049	-36.82
	H...C	2.18	0.023	0.055	-0.0046	

\*  $E_{\text{int}} = E_{\text{Hyd@MF}} - E_{\text{Hyd}} - E_{\text{MF}} + \text{BSSE}$ .

**Table 2**

The evaluated thermochemistry features of singular Hyd and MF models and interacting Hyd@MF complexes.\*

Model	$E + G$ (au)	$\Delta[E + G]$ (au)	$E + H$ (au)	$\Delta[E + H]$ (au)	S (Cal/mol.K)	$\Delta[S]$ (Cal/mol.K)
Hyd	-300.38		-300.35		71.98	
FeF	-1986.88		-1986.84		91.23	
NiF	-2231.45		-2231.40		92.88	
ZnF	-2502.43		-2502.38		92.20	
Hyd@FeF	-2287.30	-0.0372	-2287.24	-0.0536	128.60	-34.61
Hyd@NiF	-2531.87	-0.0375	-2531.80	-0.0547	128.48	-36.38
Hyd@ZnF	-2802.84	-0.0388	-2802.78	-0.0568	126.33	-37.85

\*  $\Delta[X] = X_{\text{Hyd@MF}} - X_{\text{Hyd}} - X_{\text{MF}}$ .**Table 3**

The evaluated FMO features of singular Hyd and MF models and interacting Hyd@MF complexes.\*

Model	HOMO (eV)	LUMO (eV)	$E_{\text{gap}}$ (eV)	$C_{\text{pot}}$ (eV)	$C_{\text{hard}}$ (eV)
Hyd	-6.97	0.95	7.92	-3.01	3.96
FeF	-5.03	-2.85	2.18	-3.94	1.09
NiF	-5.28	-3.63	1.65	-4.56	0.82
ZnF	-6.02	-2.97	3.05	-4.49	1.52
Hyd@FeF	-4.36	-2.28	2.08	-3.32	1.04
Hyd@NiF	-4.63	-2.81	1.82	-3.72	0.91
Hyd@ZnF	-5.42	-2.43	2.99	-3.92	1.49

\*  $E_{\text{gap}} = \text{LUMO} - \text{HOMO}$ ;  $C_{\text{pot}} = \frac{1}{2} (\text{LUMO} + \text{HOMO})$ ;  $C_{\text{hard}} = \frac{1}{2} (\text{LUMO} - \text{HOMO})$ .

managing the interactions and formations of the corresponding complexes to each model. In this case, the Zn atom showed the highest contribution to the management of O...M interaction, in which the H value of QTAIM analyses was found -0.49 au for the O...Zn interaction. The next orders were found for Ni and Fe, respectively, with the H value of -0.46 au and -0.45 au, in which the complex strengths were ordered based on such a dominant role of metal-doping atom as Hyd@ZnF > Hyd@NiF > Hyd@FeF complexes. The benefit of this achievement could return to the importance of customizing nanostructures for achieving a specific application and featured properties, in which the cases of metal-doping models indicated different levels of stabilities for the Hyd@MF complex formations. Moreover, the formation of models in the direction of  $\text{Hyd} + \text{MF} \rightarrow \text{Hyd@MF}$  was found suitable by the evaluated thermochemistry features (**Table 2**). The negative values of  $\Delta[E + G]$  and  $\Delta[E + H]$  indicated an exothermic process, in which the negative values of  $\Delta[S]$  indicated a lower disorder for the complex models in comparison with the sum of counterparts. Accordingly, the Hyd@MF complex model formations were achievable based on the involved non-covalent interactions between the interacting Hyd and MF counterparts.

The frontier molecular orbital (FMO) features of singular models and complexes were summarized in **Table 3** and the illustrated DOS diagrams and HOMO-LUMO distribution patterns were exhibited in **Fig. 2**. Energy levels of HOMO and LUMO imply for the facing full and vacant molecular orbital levels of FMO, in which they can manage the important electronic behaviors and properties of a molecular model system. One of the main things of HOMO-LUMO levels is their role for working in the electron transferring mechanism inside and outside of the molecular system. Accordingly, exact energies of those levels and their related features are very important to be known for approaching the purpose of electronic characterization of a molecular system. As indicated in **Table 3**, the first impact of metal-doping enhancement was bringing different HOMO and LUMO levels for the singular MF models. Next, the complex models were also experiencing different levels of HOMO-LUMO regarding their singular counterparts and among the complexes. This observation could be related to the importance of variation monitoring of FMO levels to reveal the electronic information of investigated models. In this regard, changes of such levels could lead to providing a distinguishability of models from each other and also the sensitivity of such detection and recognition. In the case of developing

sensor materials, such electronic features could help how to manage the recognition system and how to make a sensing function for the desired purpose. In the drug delivery issues, a recognition ability is essential for the carrier how to make sense the uploaded drug and how to control it for participating in further actions and reactions. As a result, such FMO features should be learned carefully for the models of drug delivery related issues.

The energy distance of HOMO-LUMO levels is known as the energy gap ( $E_{\text{gap}}$ ), in which its smaller and larger values could reveal a higher and a lower conductivity for the investigated model. As described in **Table 3**, different values of  $E_{\text{gap}}$  were found for the singular models; FeF (2.18 eV), NiF (1.65 eV), and ZnF (3.05 eV), showing different electronic behaviors of models in the singular state due to the metal-doping enhancement. In accordance with the values of HOMO-LUMO levels and  $E_{\text{gap}}$ , the values of chemical potential ( $C_{\text{pot}}$ ) and chemical hardness ( $C_{\text{hard}}$ ) were found for the models showing the smallest value of  $C_{\text{hard}}$  for the NiF model as its  $E_{\text{gap}}$  was also the smallest one. From the singular state to the complex states, it was interesting that the models showed different behaviors as the  $E_{\text{gap}}$  values of Hyd@FeF (2.08 eV) and Hyd@ZnF (2.99 eV) were smaller than the singular FeF (2.18 eV) and ZnF (3.05 eV) models, but that of Hyd@NiF (1.82 eV) was larger than the singular NiF (1.65 eV) model. To explain what has been happening inside the models, it could be focused on different features of Fe, Ni, and Zn atoms by providing additional orbitals to the enhanced MF system. Since all the cases were in neutral zero charge and singlet spin multiplicity conditions, the models were variated because of the original features of metal atoms. To describe this issue, the illustrated DOS diagrams and HOMO-LUMO distribution patterns of models could be helpful for approaching a more clarified point of these systems. Comparing the HOMO-LUMO patterns of singular and complex states could reveal that the general shapes of FeF and ZnF models were almost similar in both states; however, the general shape of NiF model was different in the singular and complex states. Accordingly, the variation of molecular orbitals patterns from singular to complex states were also different for the NiF → Hyd@NiF mechanism in contrast with other two mechanisms; FeF → Hyd@FeF and ZnF → Hyd@ZnF. As a consequence, the effect of Ni-doping enhancement was found completely different from the effects of employed Fe-doped and Zn-doped enhancements for the investigated systems.

Even the illustrated DOS diagrams showed a significance of molecular orbitals variations before the HOMO level and after the LUMO level for both of singular and complex states of all models. For providing a sensing function for the enhanced MF substances in addition to their recovery time duration, the conductance rate variations could be learned by monitoring the variations of FMO features at the exact HOMO-LUMO levels and their surrounding levels. As a consequence, the models were suitable to be recognized by changes of FMO features, in which the highest change was found for the NiF → Hyd@NiF mechanism, in the case that the other mechanisms were still meaningful to be detected and recognized. As a consequence, the sensing functions of enhanced MF counterparts towards the Hyd anticancer were found considerable to work as promising carriers regarding the drug delivery issues. As a conclusion, the ZnF → Hyd@ZnF mechanism was highlighted for the recovery time duration and the NiF → Hyd@NiF

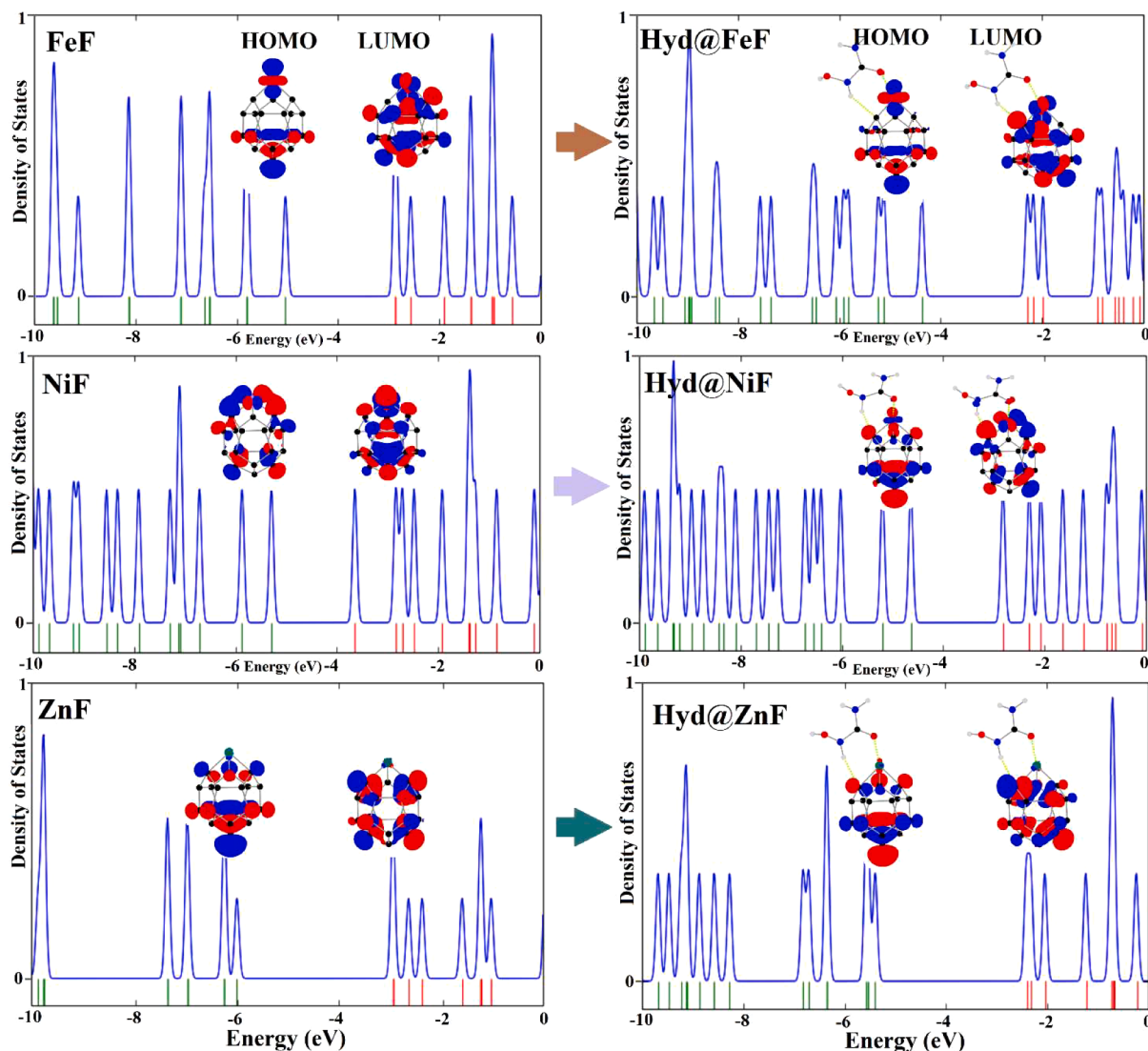


**Fig. 2.** The illustrated DOS diagrams; including HOMO-LUMO distribution patterns, of singular MF models and interacting Hyd@MF complexes.

mechanism was highlighted for the conductance rate variation; all three complexes mechanism were meaningful to be considered. Indeed, it was a prediction for both of recovery time and conductance rate based on the evaluated complex strength and energy gap features of this work whereas their exact calculations need some other parameters such as temperature. Then we tried to provide our prediction regarding these two important properties.

#### 4. Conclusion

The metal-doped fullerenes (MF) were assessed to work as promising carries of hydroxycarbamide (Hyd) anticancer along with DFT calculations. The stabilized structures were found based on the optimization calculations and their corresponding features were evaluated. The models of singular and complex states were analyzed to recognize the structural and electronic features for approaching the points of recovery time duration and conductance rate variation. To this aim, the results could be highlighted into some issues. First, the formation stability of Hyd@MF complexes were arranged as  $\text{Hyd@ZnF} > \text{Hyd@NiF} > \text{Hyd@FeF}$ . Second, the issue of recovery time duration was the longest for the  $\text{Hyd@ZnF}$  complex. Third, all complexes were involving two interactions from the Hyd side to the MF side; O...M and H...C, with the highest significance for the interactions of  $\text{Hyd@ZnF}$  complex. Fourth,

the electronic features of singular models indicated different impacts of metal-doping enhancement regarding the FMO features, in which the NiF model was found by the highest reactivity. Fifth, the  $\text{MF} \rightarrow \text{Hyd@MF}$  mechanism was found with the highest significance of electronic variations for the  $\text{NiF} \rightarrow \text{Hyd@NiF}$  mechanism indicating the highest conductance rate change for the  $\text{Hyd@NiF}$  complex formation. Sixth, the metal-doping enhancement converted the MF models very useful to work as promising carriers of Hyd anticancer regarding their structural and electronic features and monitoring the variations. As a final summarization of this work, it could be mentioned that the investigated molecular models provided insights into the drug carrier development of Hyd anticancer at the smallest scale for learning the nature of drug-carrier complex formations. The non-covalent interacting environment revealed a possibility of managing a reversible drug delivery process to successfully deliver the loaded drug to a specific target. Hence, further investigations on the investigated models could be proposed for achieving the successful results.

#### CRediT authorship contribution statement

**M.M. Salem-Bekhit:** Conceptualization, Funding acquisition, Writing – original draft. **S. Al Zahrani:** Data curation, Writing – review & editing. **N.A. Alhabib:** Formal analysis, Investigation. **R.R. Maaliw**

**III: Data curation, Software, Visualization. M. Da'i:** Conceptualization, Project administration, Writing – review & editing. **M. Mirzaei:** Investigation, Methodology, Validation.

### Declaration of Competing Interest

The authors declare that they have no known competing financial interests or personal relationships that could have appeared to influence the work reported in this paper.

### Data availability

Data will be made available on request.

### Acknowledgments

The authors extend their appreciation to the Deputyship for Research & Innovation, Ministry of Education in Saudi Arabia for funding this research (IFKSURC-1-0802).

### References

- [1] A. Garg, H.K. Dewangan, Recent advances in drug design and delivery across biological barriers using computational models, *Lett. Drug Des. Discov.* 19 (2022) 865.
- [2] A.Y. Mohammed, L.S. Ahamed, Synthesis and characterization of new substituted coumarin derivatives and study their biological activity, *Chem. Methodol.* 6 (2022) 813.
- [3] Q. Kadhim, A. Alfalluji, F. Essa, Characterization of nanofibrous scaffolds for nanomedical applications involving poly (methyl methacrylate)/poly (vinyl alcohol), *J. Med. Pharm. Chem. Res.* 5 (2023) 720.
- [4] Y. Yao, Y. Zhou, L. Liu, Y. Xu, Q. Chen, Y. Wang, S. Wu, Y. Deng, J. Zhang, A. Shao, Nanoparticle-based drug delivery in cancer therapy and its role in overcoming drug resistance, *Front. Mol. Biosci.* 7 (2020) 193.
- [5] S.A. Mosaddad, A. Hussain, H. Tebyaniyan, Green alternatives as antimicrobial agents in mitigating periodontal diseases: a narrative review, *Microorganisms* 11 (2023) 1269.
- [6] S.M. Abdulghani, M.S. Al-Rawi, J.H. Tomma, Synthesis of new 1,2,4-triazole derivatives with expected biological activities, *Chem. Methodol.* 6 (2022) 59.
- [7] A. Mokhtari Ardekan, S. Mohammadzadehsaliani, H. Behrouj, H. Moridi, M. N. Moradi, H. Ghasemi, miR-122 dysregulation is associated with type 2 diabetes mellitus-induced dyslipidemia and hyperglycemia independently of its rs17669 variant, *Mol. Biol. Rep.* 50 (2023) 4217.
- [8] M. Naeimi Darestani, H. Asl Roosta, S.A. Mosaddad, S. Yaghoubi, The effect of leukocyte- and platelet-rich fibrin on the bone loss and primary stability of implants placed in posterior maxilla: a randomized clinical trial, *Int. J. Implant Dent.* 9 (2023) 23.
- [9] D. Sharma, G. Singh Aujla, R. Bajaj, Evolution from ancient medication to human-centered Healthcare 4.0: a review on health care recommender systems, *Int. J. Commun. Syst.* 36 (2023) e4058.
- [10] K. Nasiri, S. Mohammadzadehsaliani, H. Kheradjoo, A.M. Shabestari, P. Eshaghizadeh, A. Pakmehr, M.F. Alsaffar, B.Z. Al-Naqeeb, S. Yasmineh, O. Gholizadeh, Spotlight on the impact of viral infections on hematopoietic stem cells (HSCs) with a focus on COVID-19 effects, *Cell Commun. Signaling* 21 (2023) 102.
- [11] S.A. Mosaddad, A. Hussain, H. Tebyaniyan, Exploring the use of animal models in craniofacial regenerative medicine: a narrative review, *Tissue Eng. Part B Rev.* (2023).
- [12] S.A. Mosaddad, P. Mahootchi, S. Safari, H. Rahimi, S.S. Aghili, Interactions between systemic diseases and oral microbiota shifts in the aging community: a narrative review, *J. Basic Microbiol.* 63 (2023) 831.
- [13] A. Umar, S.H. Abdullahi, A. Uzairu, G. Shallangwa, S. Uba, Molecular docking studies of some coumarin derivatives as anti-breast cancer agents: computer-aided design and pharmacokinetics studies, *Prog. Chem. Biochem. Res.* 6 (2023) 229.
- [14] N. Asghari, S. Houshmand, A. Rigi, V. Mohammadzadeh, M. Piri Dizaj, Z. S Mousavian Hiagh, PEGylated cationic nano-niosomes formulation containing herbal medicine curcumin for drug delivery to MCF-7 breast cancer cells, *J. Med. Pharm. Chem. Res.* 5 (2023) 556.
- [15] S. Maghsoudi, S.A. Hosseini, S. Ravandi, A review on phospholipid and liposome carriers: synthetic methods and their applications in drug delivery, *J. Chem. Rev.* 4 (2022) 346.
- [16] H. Ahmed, S.S. Gomte, E. Prathyusha, A. Prabakaran, M. Agrawal, A Alexander, Biomedical applications of mesoporous silica nanoparticles as a drug delivery carrier, *J. Drug Deliv. Sci. Technol.* 76 (2022), 103729.
- [17] M.M. Salem-Bekhit, M. Da'i, M.M. Rakhatullaeva, M. Mirzaei, S. Al Zahrahi, N. Alhabib, The drug delivery of methimazole through the sensing function assessments of BeO fullerene-like particles: DFT study, *Chem. Phys. Impact* 7 (2023), 100335.
- [18] G.R. Ortiz, B. Cespedes-Panduro, I. Saba, J.C. Cotrina-Aliaga, M. Mohany, S.S. Al-Rejaie, J.L. Arias-Gonzales, A.A. Ramiz-Cornell, M.J. Kadham, R. Akhavan-Sigari, Adsorption of thioptera anticancer by the assistance of aluminum nitride nanocage scaffolds: a computational perspective on drug delivery applications, *Colloids Surf. A Physicochem. Eng. Asp.* 666 (2023), 131276.
- [19] J.A. Finbloom, F. Sousa, M.M. Stevens, T.A. Desai, Engineering the drug carrier biointerface to overcome biological barriers to drug delivery, *Adv. Drug Deliv. Rev.* 167 (2020) 89.
- [20] H. Darougari, M. Rezaei-Sameti, The drug delivery appraisal of Cu and Ni decorated B12N12 nanocage for an 8-hydroxyquinoline drug: a DFT and TD-DFT computational study, *J. Med. Nanomat. Chem.* 4 (2022) 196.
- [21] F. Zare Kazemabadi, A. Heydarinasab, A. Akbarzadehkhiyavi, M Ardjamand, Development, optimization and in vitro evaluation of etoposide loaded lipid polymer hybrid nanoparticles for controlled drug delivery on lung cancer, *Chem. Methodol.* 5 (2021) 135.
- [22] Y. Wang, R. Cai, C. Chen, The nano-bio interactions of nanomedicines: understanding the biochemical driving forces and redox reactions, *Acc. Chem. Res.* 52 (2019) 1507.
- [23] R. Shete, P. Fernandes, B. Borhade, A. Pawar, M. Sonawane, N. Warude, Review of cobalt oxide nanoparticles: green synthesis, biomedical applications, and toxicity studies, *J. Chem. Rev.* 4 (2022) 331.
- [24] A. Belhachem, N. Amara, H. Belmekki, Y. Yahia, Z. Cherifi, A. Amari, A. Bengueddach, R. Meghabar, H. Toumi, Synthesis, characterization and anti-inflammatory activity of an alginate-zinc oxide nanocomposite, *J. Med. Nanomat. Chem.* 5 (2023) 173.
- [25] G. Qu, T. Xia, W. Zhou, X. Zhang, H. Zhang, L. Hu, J. Shi, X.F. Yu, G. Jiang, Property–activity relationship of black phosphorus at the nano-bio interface: from molecules to organisms, *Chem. Rev.* 120 (2020) 2288.
- [26] Y. Hu, C.M. Niemeyer, From DNA nanotechnology to material systems engineering, *Adv. Mater.* 31 (2019), 1806294.
- [27] V. Daghighe, T.E. Lacy Jr, H. Daghighe, G. Gu, K.T. Baghaei, M.F. Horstemeyer, C. U Pittman Jr, Machine learning predictions on fracture toughness of multiscale bio-nano-composites, *J. Reinf. Plast. Compos.* 39 (2020) 587.
- [28] R.D. Pecho, N. Hajali, R.D. Tapia-Silguera, L. Yassen, M. Alwan, M.J. Jawad, F. Castro-Cayllahua, M. Mirzaei, R. Akhavan-Sigari, Molecular insights into the sensing function of an oxidized graphene flake for the adsorption of avigan antiviral drug, *Comput. Theor. Chem.* 1227 (2023), 114240.
- [29] M.J. Saadh, F.A. Muhammad, R. Mahdavi, Y. Nazariyan Parizi, E. Balali, J. Carlos Cotrina-Aliaga, M. Adil, S. Ahjel, M. Tania Churampi Arellano, Y. Gallardo-Lolandes, R.R. Maaliw III, M. Mirzaei, K Harismah, Exploring impacts of oil and water environments on structural and electronic features of vitamin B3 along with DFT calculations, *J. Med. Chem. Sci.* 6 (2023) 2419.
- [30] M. Da'i, Wahyuni AS Maryati, E.R. Wikantyasnig, M Mirzaei, Vitamin-B3 adsorption by a Ti-doped graphene, *Biointerface Res. Appl. Chem.* 13 (2023) 482.
- [31] R.C. Donehower, An overview of the clinical experience with hydroxyurea, *Semin. Oncol.* 19 (1992) 11.
- [32] K. Madaan, D. Kaushik, T. Verma, Hydroxyurea: a key player in cancer chemotherapy, *Expert Rev. Anticancer Ther.* 12 (2012) 19.
- [33] M.E. Fields, K.P. Guilliams, D. Ragan, M.M. Binkley, A. Mirro, S. Fellah, M. L. Hulbert, M. Blinder, C. Eldeniz, K. Vo, J.S. Shimony, Hydroxyurea reduces cerebral metabolic stress in patients with sickle cell anemia, *Blood* 133 (2019) 2436.
- [34] A. Power-Hays, R.E Ware, Effective use of hydroxyurea for SCA in low-resource countries, *Curr. Opin. Hematol.* 27 (2020) 172.
- [35] C.A. Bulte, K.M. Hoegler, O. Kutlu, A. Khachemoune, Hydroxyurea: a reappraisal of its cutaneous side effects and their management, *Int. J. Dermatol.* 60 (2021) 810.
- [36] V. Simeonovski, H. Breshkovska, S. Duma, I. Dochcheva-Karajovanov, K. Damevska, S. Nikolovska, Hydroxyurea associated cutaneous lesions: a case report, *Open Access Maced. J. Med. Sci.* 6 (2018) 1458.
- [37] O.A. Alvarez, S. Echenique, E.L. Clay, H. Rodriguez-Cortes, T.J. Harrington, M. E. Berry, M. Murph, C. Wells, C. Courtlandt, L. Noonan, Successful quality improvement projects to maximize prescription rates and acceptance of hydroxyurea among patients with sickle cell anemia, *Blood* 138 (2021) 2983.
- [38] M.M. Kadhim, N. Sheibanian, D. Ashoori, M. Sadri, B. Tavakoli-Far, R. Khadivi, R. Akhavan-Sigari, The drug delivery of hydrea anticancer by a nanocone-oxide: computational assessments, *Comput. Theor. Chem.* 1215 (2022), 113843.
- [39] M. Da'i, A.S. Wahyuni, E.R. Wikantyasnig, Mirzaei M Maryati, Insights into the delivery of hydrea anticancer drug by the assistance of an oxidized silicon carbide nanocage, *Biointerface Res. Appl. Chem.* 13 (2023) 497.
- [40] K. Harismah, A. Hassan, O.T. Hamid, M.A. Saadoon, H. Zandi, Drug delivery assessments of hydroxyurea anticancer by an epoxy-decorated fullerene cage, *Biointerface Res. Appl. Chem.* 13 (2023) 392.
- [41] K. Harismah, D.K. Sain, Al-Owaidi MF, H. Zandi, A. Saimmai, Assessing a BN-doped graphene for the drug delivery of hydroxyurea anticancer, *Biointerface Res. Appl. Chem.* 13 (2023) 485.
- [42] A. Omid, R. Esmkhani, Study of chemical activity and adsorption properties of boron nitride nanocagesInteraction with hydroxycarbamide anticancer drug by density functional theory method, *Nanoscale* 6 (2019) 11.
- [43] M.S. Khanom, M.R. Hossain, K.Z. Islam, M.A. Hossain, F. Ahmed, First-principles investigation of Hydroxycarbamide anticancer drug delivery by X12N12 (X= B, Al, Ga) fullerene nanostructures: a DFT, NBO and QTAIM analysis, *Comput. Theor. Chem.* 1216 (2022), 113869.
- [44] C.G. Apebende, H. Louis, A.E. Owen, I. Benjamin, I.O. Amodu, T.E. Gber, F. C. Asogwa, Adsorption properties of metal functionalized fullerene (C59Au, C59Hf, C59Ag, and C59Ir) nanoclusters for application as a biosensor for hydroxyurea (HXU): insight from theoretical computation, *Z. Phys. Chem.* 236 (2022) 1515.

- [45] S. Esfahani, J. Akbari, S. Soleimani-Amiri, M. Mirzaei, A. Ghasemi Gol, Assessing the drug delivery of ibuprofen by the assistance of metal-doped graphenes: insights from density functional theory, *Diam. Relat. Mater.* 135 (2023), 109893.
- [46] L.M. Al-Haideri, N. Cakmak, DFT calculations of structural and electronic features for mono and dual Pb-doped models of graphene, *Indian J. Phys.* 96 (2022) 2795.
- [47] R.U. Shenoy, A. Rama, I. Govindan, A. Naha, The purview of doped nanoparticles: insights into their biomedical applications, *OpenNano* 8 (2022), 100070.
- [48] V. Chandrakala, V. Aruna, G. Angajala, Review on metal nanoparticles as nanocarriers: current challenges and perspectives in drug delivery systems, *Emergent Mater.* 5 (2022) 1593.
- [49] Y. Sun, J. Zhu, Y. Chen, Metal-fullerene assisted adsorption of dichlorosilane: DFT assessments, *Comput. Theor. Chem.* 1216 (2022), 113868.
- [50] L. Liu, A. He, Z. Yuan, Methylene blue adsorption by metal-decorated fullerenes: DFT assessments, *Comput. Theor. Chem.* 1214 (2022), 113803.
- [51] G. Chala, Review on green synthesis of iron-based nanoparticles for environmental applications, *J. Chem. Rev.* 5 (2023) 1.
- [52] S.N. Bhatia, X. Chen, M.A. Dobrovolskaia, T. Lammers, Cancer nanomedicine, *Nat. Rev. Cancer* 22 (2022) 550.
- [53] H. Haryoto, Cytotoxic activities of ethanol extract, nonpolar semipolar, and polar fractions of *Dioscorea esculenta* L.) on MCF7 cancer cell, *J. Nutraceuticals Herbal Med.* 2 (2019) 12.
- [54] S. Kasim, N. Abdulaziz, M. Jasim, Y. Mustafa, Resveratrol in cancer chemotherapy: is it a preventer, protector, or fighter? *J. Med. Pharm. Chem. Res.* 5 (2023) 576.
- [55] D. Hudyawati, W. Syafitry, Effectiveness of physical and psychological treatment for cancer-related fatigue: systematic review, *J. Kesehatan* 14 (2021) 195.
- [56] Q. Wang, P. Zhang, M.J. Ansari, M.F. Aldawsari, A.S. Alalaiwe, J. Kaur, R. Kumar, A.N. Lup, A. Enayati, H. Mirzaei, A. Soltani, Electrostatic interaction assisted Ca-decorated C20 fullerene loaded to anti-inflammatory drugs to manage cardiovascular disease risk in rheumatoid arthritis patients, *J. Mol. Liq.* 350 (2022), 118564.
- [57] Ö. Alver, C. Parlak, Y. Umar, P. Ramasami, DFT/QTAIM analysis of favipiravir adsorption on pristine and silicon doped C20 fullerenes, *Main Group Metal Chem.* 42 (2019) 143.
- [58] R.F. Bader, T.T. Nguyen-Dang, Quantum theory of atoms in molecules–Dalton revisited, *Adv. Quantum Chem.* 14 (1981) 63.
- [59] M. Ghiasifar, T. Hosseininejad, A. Ahangar, Copper catalyzed cycloaddition reaction of azidomethyl benzene with 2,2-di(prop-2-yn-1-yl)propane-1,3-diol: DFT and QTAIM investigation, *Prog. Chem. Biochem. Res.* 5 (2022) 1.
- [60] E.R. Davidson, S.J. Chakravorty, A possible definition of basis set superposition error, *Chem. Phys. Lett.* 217 (1994) 48.
- [61] M.J. Frisch, G.W. Trucks, H.B. Schlegel, G.E. Scuseria, M.A. Robb, J.R. Cheeseman, et al., *Gaussian 09 Program*, Gaussian Inc, Wallingford, CT, 2009.
- [62] M. Walker, A.J. Harvey, A. Sen, C.E. Dessent, Performance of M06, M06-2X, and M06-HF density functionals for conformationally flexible anionic clusters: M06 functionals perform better than B3LYP for a model system with dispersion and ionic hydrogen-bonding interactions, *J. Phys. Chem. A* 117 (2013) 12590.
- [63] V.A. Rassolov, M.A. Ratner, J.A. Pople, P.C. Redfern, L.A. Curtiss, 6-31G\* basis set for third-row atoms, *J. Comput. Chem.* 22 (2001) 976.
- [64] T. Lu, F. Chen, Multivfn: a multifunctional wavefunction analyzer, *J. Comput. Chem.* 33 (2012) 580.
- [65] N.M. O'boyle, A.L. Tenderholt, K.M. Langner, cclib: A library for package-independent computational chemistry algorithms, *J. Comput. Chem.* 29 (2008) 839.
- [66] ChemCraft - graphical software for visualization of quantum chemistry computations. Version 1.8, build 654 <https://www.chemcraftprog.com>.
- [67] M.J. Saadh, M. Mirzaei, B.S. Abdullaeva, R.R. Maaliw III, M. Da'i, M.M. Salem-Bekhit, R. Akhavan-Sigari, Explorations of structural and electronic features of an enhanced iron-doped boron nitride nanocage for adsorbing/sensing functions of the hydroxyurea anticancer drug delivery under density functional theory calculations, *Phys. B Condens. Matter* 671 (2023) 415445.

# FACULTY POSITION RECLASSIFICATION FOR SUCS

(DBM-CHED Joint Circular No. 3, series of 2022)

## CERTIFICATION OF PERCENTAGE CONTRIBUTION

(Research Output with Multiple Authors)

**Title of Research:** Metal-Dope Fullerenes as Promising Drug Carriers of Hydroxycarbamide Anticancer: Insights from Density Functional Theory

**Type of Research Output:** Journal Article (Scopus and WOS Indexed, Elsevier)

**Instruction:** Supply ALL the names of the authors involved in the publication of Research output and indicate the contribution of each author in percentage. Each author shall sign the Conforme column if he/she agrees with the distribution. The Conforme should be signed by all the authors in order to be considered. Please prepare separate Certification for each output.

	Name of Authors	Current Affiliations	% Contribution	Conforme (Sign if you agree with the % distribution)
1	M. M. Salem-Bekhit	King Saud University	16.67%	
2	S. Al Zahrani	King Saud University	16.67%	
3	N. A. Alhabib	King Saud University	16.67%	
4	Renato R. Maaliw III	SLSU	16.67%	
5	Muhammad Dai	Universitas Surakata	16.67%	
6	M. Mirzaei	Tarsus University	16.67%	
* Should have a total of 100%			100.00%	

Prepared by:

  
**Renato R. Maaliw III, DIT**  
(Name and Signature)  
Faculty

Certified by:

**Nicanor L. Guinto, Ph.D**  
(Name and Signature)  
Director, Office of Research Services